

Article

Unveiling the Past: Deep-Learning-Based Estimation of Historical Peatland Distribution

Sungeun Cha ¹, Junghee Lee ², Eunho Choi ³ and Joongbin Lim ^{2,*}¹ Forest Fire Division, National Institute of Forest Science, Seoul 02455, Republic of Korea; scha@korea.kr² Forest ICT Research Center, National Institute of Forest Science, Seoul 02455, Republic of Korea; junghee23@korea.kr³ Global Forestry Division, National Institute of Forest Science, Seoul 02455, Republic of Korea; ehchoi710@korea.kr

* Correspondence: jlim@korea.kr; Tel.: +82-2-961-2958

Abstract: Acknowledging the critical role of accurate peatland distribution estimation, this paper underscores the significance of understanding and mapping these ecosystems for effective environmental management. Highlighting the importance of precision in estimating peatland distribution, the research aims to contribute valuable insights into ecological monitoring and conservation efforts. Prior studies lack robust validation, and while recent advancements propose machine learning for peatland estimation, challenges persist. This paper focuses on the integration of deep learning into peatland detection, underscoring the urgency of safeguarding these global carbon reservoirs. Results from convolutional neural networks (CNNs) reveal a decrease in the classified peatland area from 8226 km² in 1999 to 5156 km² in 2019, signifying a 37.32% transition. Shifts in land cover types are evident, with an increase in estate plantation and a decrease in swamp shrub. Human activities, climate, and wildfires significantly influenced these changes over two decades. Fire incidents, totaling 47,860 from 2000 to 2019, demonstrate a substantial peatland loss rate, indicating a correlation between fires and peatland loss. In 2020, wildfire hotspots were predominantly associated with agricultural activities, highlighting subsequent land cover changes post-fire. The CNNs consistently achieve validation accuracy exceeding 93% for the years 1999, 2009, and 2019. Extending beyond academic realms, these discoveries establish the foundation for enhanced land-use planning, intensified conservation initiatives, and effective ecosystem management—a necessity for ensuring sustainable environmental practices in Indonesian peatlands.

Keywords: peatland detection; peatland loss; deep learning; convolutional neural networks (CNNs); multi-temporally integrated satellite imageries; land cover change



Citation: Cha, S.; Lee, J.; Choi, E.; Lim, J. Unveiling the Past: Deep-Learning-Based Estimation of Historical Peatland Distribution. *Land* **2024**, *13*, 328. <https://doi.org/10.3390/land13030328>

Academic Editor: Juan Infante Amate

Received: 11 October 2023
Revised: 10 November 2023
Accepted: 16 November 2023
Published: 4 March 2024



Copyright: © 2024 by the authors. Licensee MDPI, Basel, Switzerland. This article is an open access article distributed under the terms and conditions of the Creative Commons Attribution (CC BY) license (<https://creativecommons.org/licenses/by/4.0/>).

1. Introduction

Peatlands, comprising a mere 3% of the Earth's land surface [1], hold unparalleled importance as natural carbon reservoirs, safeguarding over 31% of the planet's terrestrial carbon reserves [2]. In Indonesia, the Ministry of Agriculture defines 'peat' as soil formed due to the accumulation of organic matter, with a naturally occurring composition of more than 65% from decaying vegetation growing on it, where decomposition is slowed down by anaerobic and wet conditions. Despite their seemingly modest footprint, these ecosystems serve as indispensable carbon sinks, playing a pivotal role in mitigating climate change. Nonetheless, the existence of these ecosystems is at risk due to the unyielding progression of climate change and the destructive consequences of wildfires [3,4], endangering the stability of peatlands and causing the emission of carbon sequestered for centuries into the atmosphere.

Wildfires in peatlands, arising from a convergence of human activities and natural factors, demand attention. The 2015 wildfire alone consumed 2.6 million hectares, including valuable peatlands, contributing to approximately 5% of CO₂ emissions from global

fossil fuel sources [5]. Extensive deforestation and drainage for small-scale agriculture in Indonesian peatlands have heightened their vulnerability to land use changes [6–8]. The practice of Manusul, involving land clearing, sometimes triggers unintentional fires beyond firebreaks during dry seasons [9]. Prolonged periods of arid conditions heighten the vulnerability to ignition, with climate phenomena such as the El Niño Southern Oscillation and the Indian Ocean Dipole serving as pivotal influencers of fire incidence [10,11]. These sudden events alter peatland distributions, necessitating vigilant monitoring of peatland change patterns.

The imperative for action extends beyond comprehending the present condition of peatlands; it requires a vigilant gaze capable of discerning nuanced changes over time. Conventional field-based assessments, while commendable, demand substantial resources. However, the fusion of satellite imagery with advanced deep learning techniques represents a groundbreaking advancement in peatland analysis and conservation [12,13]. This collaboration unlocks scalable and accurate peatland detection capabilities, providing a transformative approach to efficient peatland management. Influenced by the intricate interplay between climate and topography, accurately delineating the spatial distribution of peatlands poses a significant challenge. To tackle this complex puzzle, [14] proposed the creation of a global PEATMAP, leveraging a comprehensive meta-analysis of diverse geospatial information. Their estimation of the global peatland area, a staggering 4.23 million km², suggested potential underestimations in tropical regions and overestimations in mid-latitudes, stemming from a lack of actual data or reliance on limited information such as organic soil content.

While previous studies have attempted to map peatlands through field observations and remote sensing images, a critical gap exists in the lack of robust validation and uncertainty analyses [15]. For example, the comprehensive work of [16]—employing various data sources, including optical and SAR sensors, alongside field survey data—revealed peatland areas in Sumatra, Kalimantan, Papua, and Sulawesi. This provides a regional perspective, but also underscores the need for precision in mapping. In the wake of technological leaps, recent advancements propose peatland estimation technology using machine learning [12,13,17]. However, delving into this domain is riddled with challenges, primarily the formidable task of acquiring ground-referenced data. Consequently, only a limited number of investigations have been reported, emphasizing the pioneering nature of this field and the uncharted potential awaiting in-depth exploration.

This paper embarks on a profound journey into the realm of deep learning, exploring its integration into peatland detection using satellite imagery. The primary objective is to accurately predict peatland and understand its distribution changes. At its core, our research is rooted in a deep appreciation for peatlands, viewing them not only as enigmatic ecosystems, but also as crucial carbon reservoirs of global significance, essential for sustaining life. Highlighting the importance of conserving these vital carbon reserves, we face persistent environmental challenges, strongly advocating for the integration of state-of-the-art technology and ecological knowledge. Our mission is to safeguard the Earth's seemingly modest yet priceless carbon custodians, constructing a narrative that extends beyond scientific inquiry to underscore the imperative nature of ecological stewardship.

2. Materials and Methods

2.1. Study Sites

The Ogan Komering Ilir (OKI) region in Indonesia is characterized by a blend of geographical and climatic features, with a noteworthy focus on its prominent peatland areas (Figure 1). The OKI region situated within the South Sumatra Province is positioned between 2°30'–4°15' South Latitude and 104°20'–106°00' East Longitude. Situated in the southern expanse of Sumatra Island, this region encompasses varied topography, ranging from expansive low-lying plains to undulating hills. One of the most distinctive attributes of this region lies in its extensive peatlands. Indonesian peatlands are predominantly composed of humic gravel and organic soil, intricately linked to the region's hydrological

dynamics. Humic gravel, rich in organic content, shapes the soil composition and plays a crucial role in fertility, providing essential nutrients for plant growth. Organic soil results from the accumulation of decomposed plant material in waterlogged environments, contributing to the unique characteristics of peatlands, including their high carbon content. Additionally, the extensive wetland coverage is a distinctive feature shaping the physical landscape of the region [18]. A substantial portion of the region, totaling around 768,501 ha, is occupied by peatlands. Remarkably, this constitutes 50.6% of the entire peatland area within South Sumatra Province. These peatlands developed over centuries through the gradual accumulation of partially decomposed plant materials [18].

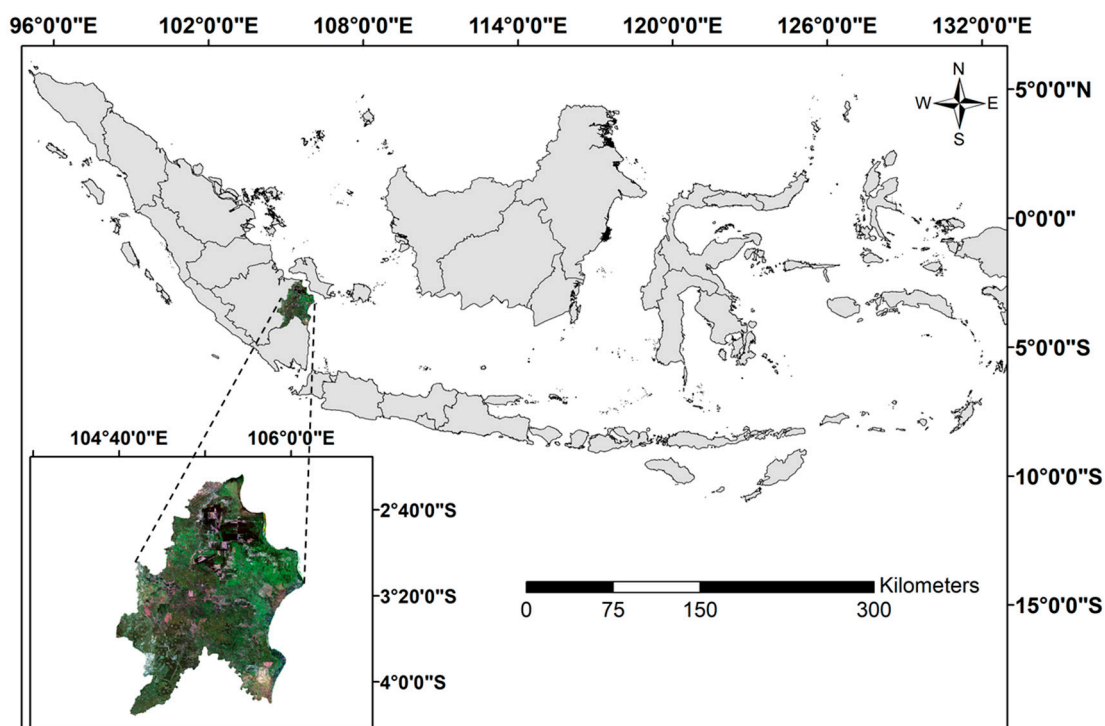


Figure 1. Boundary of study area, Ogan Komering Ilir (OKI) region.

Shifting our focus to the climate, OKI experiences a tropical climate that showcases distinct wet and dry seasons. The wet season, spanning from November to March, is characterized by abundant rainfall and heightened humidity levels. The region is often serenaded by frequent downpours and occasional thunderstorms during this period, which replenishes water bodies, rejuvenates vegetation, and bestows a refreshing ambiance. Conversely, the dry season, spanning from April to October, introduces a different facet of the climate. During this phase, precipitation is reduced, and the humidity levels tend to decrease. Skies become clearer, and temperatures experience a relative dip. This dry interlude can sometimes manifest as drought conditions, affecting the local ecosystems, water availability, and agriculture. Furthermore, this area experiences a tropical climate characterized by a distinct dry season spanning from April to September, followed by a wet season from October to March. The annual precipitation varies between 2600 and 2900 mm, complemented by an average temperature of approximately 31 °C [19].

2.2. Input Dataset

In this study, we conducted the preprocessing of Landsat 5 and 8 satellite imageries using the SEPAL platform, which was made available by the Food and Agriculture Organization (FAO) and can be accessed at <https://sepal.io> (accessed on 1 November 2023). Preprocessing involves geometric correction, orthorectification, atmospheric correction, radiometric calibration, and cloud masking. We derived the common bands for Landsat 5

and 8, which included blue, green, red, near-infrared (NIR), shortwave infrared 1 (SWIR-1), shortwave infrared 2 (SWIR-2), and wetness bands.

To extract vegetation features from the satellite imagery, we employed a range of techniques that encompassed vegetation indices. The NDVI (Normalized Difference Vegetation Index) gauges the vitality of vegetation, while the NDMI (Normalized Difference Moisture Index) delves into soil moisture levels. The NDWI (Normalized Difference Water Index) distinguishes water bodies and stressed vegetation, while the MNDVI (Modified NDVI) fine-tunes for soil context. The NDFI (Normalized Difference Fraction Index) targets urban vegetation, the EVI (Enhanced Vegetation Index) refines for dense greenery, and the SAVI (Soil-Adjusted Vegetation Index) corrects for soil interference. The NBR (Normalized Burn Ratio) pinpoints fire scars, and the MVI (Moisture Vegetation Index) fuses moisture and health insights [20–27]. The digital elevation models (DEMs) play a pivotal role in peatland analysis, offering valuable insights into terrain characteristics. Among these, slope and aspect, derived from DEMs, hold remarkable significance in comprehending peatland landscapes [16]. The slope provides crucial information about the steepness of the terrain. The aspect unveils the direction in which a slope faces, shedding light on sunlight exposure, wind dynamics, and microclimate formation. Through the identification of the steepest descent direction for each cell, the aspect aids our understanding of peatland ecological processes. The integration of slope and aspect paints a comprehensive picture of peatland terrains, elucidating how variations in topography and orientations influence the intricate balance of ecosystems and human settlements within these environments [28].

This study categorized the input dataset through the wavelengths from satellite imageries, vegetation, and topographic factors that could influence peatland estimation from previous research, then analyzed the contributions of these variables [15,29–32]. This study aimed to achieve efficient peatland classification using deep learning, incorporating the derivation of permutation importance for variables. Permutation importance plays a pivotal role as a metric for evaluating variable significance. It is acquired by randomly shuffling variables to measure changes in the model's performance. If a variable notably impacts the model's predictive performance, shuffling its values results in a significant performance decrease. The process begins with the original dataset—encompassing various features—utilized to assess the model's predictive performance through metrics such as the accuracy or F1-score. Subsequently, the values corresponding to a specific feature undergo random shuffling, thereby rearranging their sequence randomly. The model is then reassessed using the shuffled data, producing a fresh measurement of predictive performance. Feature importance is quantified by assessing the divergence between the initial model performance and that achieved with the shuffled dataset. A larger divergence indicates a higher level of feature importance. This iterative process is frequently repeated multiple times to compute an average divergence, ultimately enhancing result accuracy. The insights furnished by permutation importance prove instrumental in comprehending the influence of individual features on model predictions [33].

The permutation importance values range from nearly 0 to relatively large positive values. Values closer to 0 indicate minimal variable impact on model prediction, whereas higher positive values signify a substantial influence on peatland prediction. In this study, factors with importance values surpassing 10 were identified and employed as inputs for the deep learning model. The variables with permutation importance values exceeding 10 were as follows: DEMs 30.7, NIR 19.5, MVI 15.4, MNDVI 14, and slope 10.5. These five input datasets were utilized to drive the deep learning model.

2.3. Reference Dataset

Initiated in 1905 by the Center for Agricultural Land Resources Research and Development (ICALRD), Indonesia's soil resource inventories serve diverse purposes, such as agricultural planning, erosion hazard assessments, and soil fertility monitoring. This effort has yielded an abundance of soil survey reports and maps, encompassing detailed soil profile descriptions and essential physico-chemical properties [34]. Covering the entirety of

Indonesian land, a 1:1,000,000 scale Exploration Soil Map comprises around 180 soil mapping units with 44 great groups derived from 8 orders of the US Soil Taxonomy. By 2014, comprehensive coverage extended to a 1:250,000 map encompassing all Indonesian soil.

Indonesia possesses a wealth of legacy soil data, including soil profiles, minipit observations, laboratory analyses, and polygon data with legacy soil maps and legends. This legacy information, along with maps and field data, has been instrumental in evaluating and updating the distribution of peatland across the nation. In prior studies, the estimation of peatland spatial data by [35] as well as [36] heavily relied upon the interpretation of satellite images in conjunction with land units and soil maps. These interpretations were supplemented by a limited amount of ground-based data. In regions with accessibility constraints, such as Papua, field assessments were conducted to rectify potential misclassifications identified during the initial desktop analysis. Although resource-intensive, extensive field data collection enhances estimations of diverse peatland types. Recent peatland estimates involved validating the old peatland map through ground truth data, including legacy soil information. ICALRD's peatland map update amalgamated recent soil surveys, legacy data, and auxiliary information such as digital elevation models and geological and agroclimatic maps. Overlaying existing soil observation maps with peatland maps and satellite images aids in prioritizing future soil observations and sampling strategies. When planned observations are unfeasible, priority-based selection focuses on sites lacking peat characteristic information [37].

In this study, the peatland maps generated through field surveys in 2011 and 2019 were utilized as reference values by Balai Besar Penelitian dan Pengembangan Sumber Daya Lahan Pertanian (BBSDLP) [38,39] (Figure 2). Taking limitations such as the accuracy of field survey into consideration, areas classified as peatland in both 2011 and 2019 as shown in the figure were categorized as peatland. In cases where an area was labeled as peatland in only one of the two years, it was classified as a suspected area of peatland. Furthermore, utilizing data from 18 peatland restoration projects conducted in the OKI region by the Center for International Forestry Research (CIFOR), we evaluated the accuracy of peatland distribution following peatland classification.

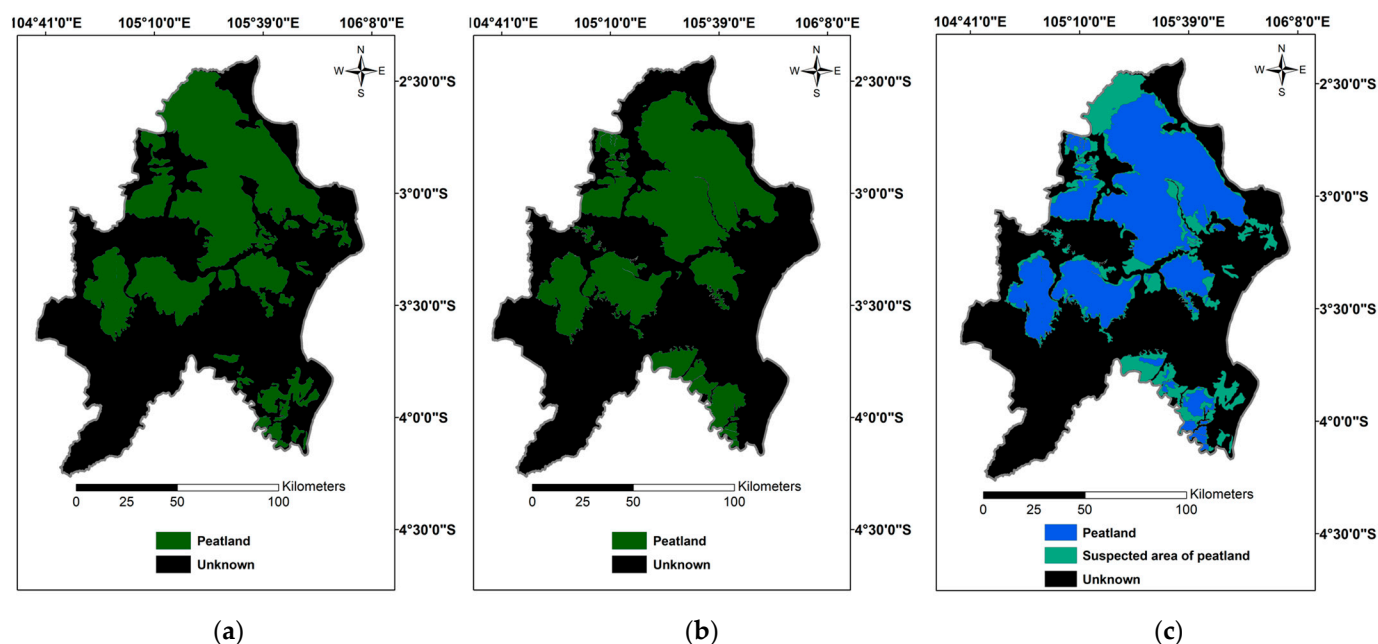


Figure 2. Peatland maps based on field survey data. (a) Peatland map for the year 2011 by BBSDLP; (b) Peatland map for the year 2019 by BBSDLP; (c) Composite peatland map for the years 2011 and 2019.

2.4. Wildfire Data from MODIS

The MODIS/Aqua+Terra Thermal Anomalies/Fire locations 1 km V0061 NRT (Near Real-Time) dataset, distributed by LANCE FIRMS (Fire Information for Resource Management System), offers a comprehensive methodology to detect and portray thermal anomalies and fire locations using vector data. This dataset leverages data from the Moderate Resolution Imaging Spectroradiometer (MODIS) instruments aboard the Aqua and Terra satellites, capturing diverse spectral bands and resolutions. The process begins by scrutinizing infrared radiation emitted from the Earth's surface. Regions exhibiting heightened thermal levels distinct from background values are pinpointed as thermal anomalies, which could potentially signify fire outbreaks [40].

Employing vector data enhances the precision in delineating areas affected by fires and thermal anomalies, yielding a deeper comprehension of their effects on the landscape. Consequently, the MODIS/Aqua+Terra Thermal Anomalies/Fire locations 1 km V0061 NRT dataset plays a pivotal role in advancing fire monitoring, environmental evaluation, and strategic land management. This dataset's insights enable us to grasp the potential impact of fire incidents on peatlands, which are highly susceptible to such disturbances due to their unique hydrological and ecological characteristics. By identifying and analyzing thermal anomalies indicative of fire, we can better understand the dynamics of peatland vulnerability, degradation, and recovery. This dataset offers valuable information for decision-makers, researchers, and land managers striving to protect and sustain peatland ecosystems.

2.5. Land Cover Map from Indonesian Ministry of Environment and Forestry (MoEF)

The land cover map provided by the Indonesian Ministry of Environment and Forestry (MoEF) is a comprehensive representation of the different types of land cover across the country. It serves as a valuable resource for understanding the spatial distribution and characteristics of various land cover categories, such as mangrove forest, swamp forest, plantation forest, bush/shrub, estate crop plantation, settlement area, bare land, savannah, water bodies, dryland agriculture, rice field, fish pond, transmigration area, and marsh. The land cover map is typically generated through the analysis of satellite imagery and remote sensing data, combined with ground-truthing and validation processes. Advanced image processing techniques are employed to classify and categorize different land cover types based on their spectral signatures, textures, and spatial patterns [41].

The Indonesian MoEF plays a crucial role in creating and distributing the land cover map, which serves as a valuable tool for informed decision-making across various levels, from local communities to national organizations. This map undergoes continuous updates and enhancements to accurately capture changes in land cover patterns over time. As a result, it offers valuable insights into the evolving landscape of Indonesia and contributes significantly to sustainable development efforts. Given its annual availability since 2000, land cover maps were utilized in this study for the years 2000, 2009, and 2019 to analyze land cover dynamics (Figure 3).

2.6. Architecture of Convolutional Neural Networks (CNNs)

Deep learning algorithms utilize artificial neural networks for "end-to-end" learning, enabling autonomous feature extraction for data analysis. This differs from traditional machine learning methods, which demand manual feature extraction based on data understanding. As data complexity grows, the strength of end-to-end deep learning becomes more pronounced.

U-net, an extension of CNNs architecture, integrates segmentation along with classification, delineating classification target boundaries [42]. The network encompasses five levels and 27 convolutional layers, organized into contracting and expansive paths. The former involves repeated 3×3 convolutions with ReLU, and 2×2 max pooling for down-sampling. The expansive path includes upsampling, 2×2 convolutions, concatenation with cropped features, and additional convolutions. The final layer maps feature vectors

to desired classes, yielding a class activation raster. This raster is compared to label raster masks (Figure 4).

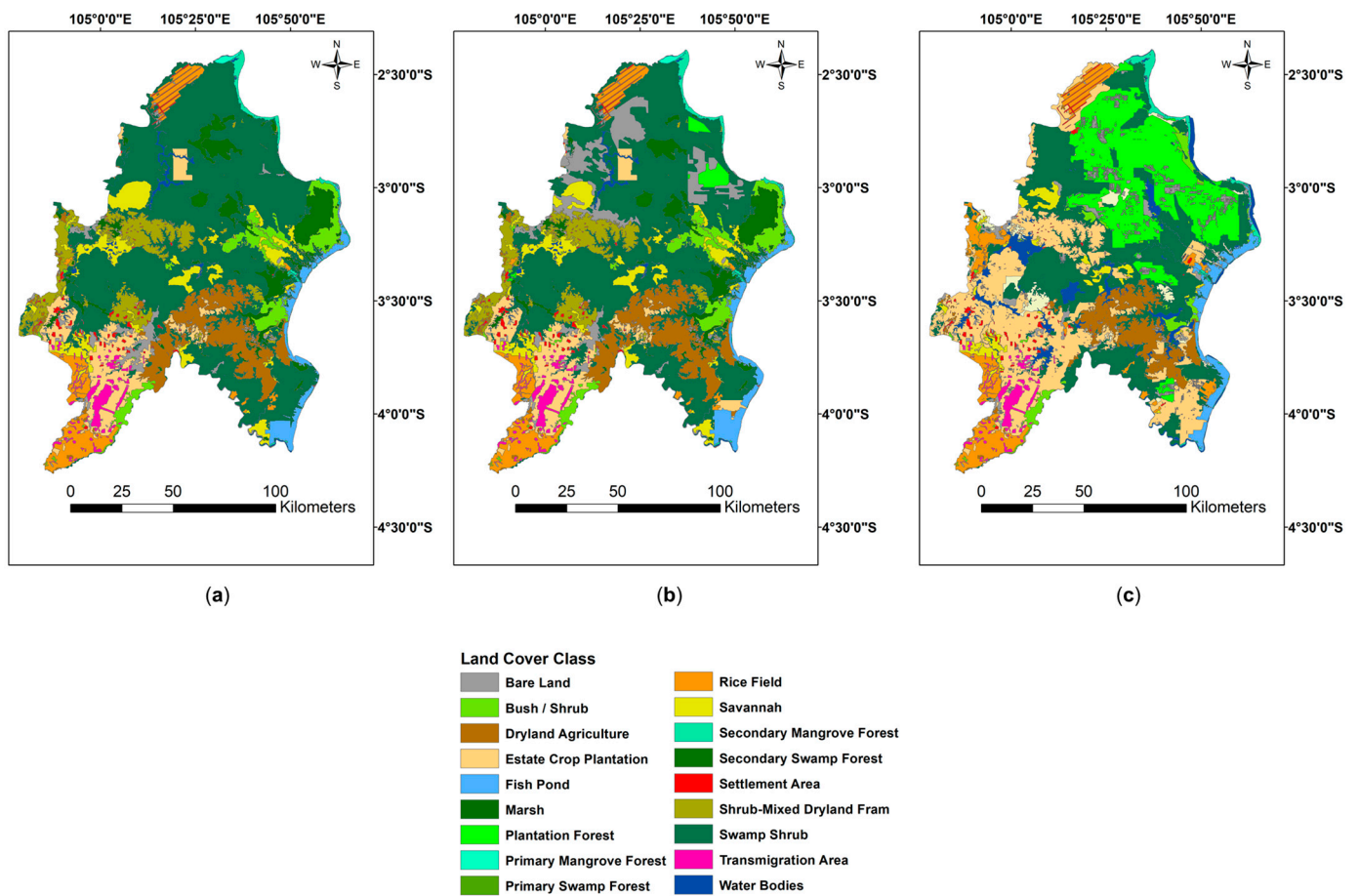


Figure 3. Land cover map. (a) Land cover map for the year 2000; (b) Land cover map for the year 2009; (c) Land cover map for the year 2019.

For machine learning, initial learning rates vary with target area size and input data resolution. Optimal learning rates are being researched [43], yet separate analyses are required for accurate modeling based on detection targets and areas. Training and validation/testing areas were divided into 70% and 30% proportions of the total study area.

2.7. Accuracy Assessment

In the assessment of tree species classification effectiveness, pivotal metrics including True Positive (TP), True Negative (TN), False Positive (FP), and False Negative (FN) were computed. TP indicates instances where both the forest type map and the convolutional neural networks (CNNs) model accurately identify the same tree species. Conversely, FN pertains to situations where both the forest type map and the CNNs model incorrectly assign different tree species compared to the reference data. Leveraging the TP , TN , FP , and FN values facilitated a comprehensive evaluation encompassing accuracy, precision, recall, f_1 score, and intersection over union (IoU). This encompassed the application of Equations (1)–(5) to derive insightful metrics that illuminate the performance of the classification process.

$$Accuracy = \frac{TP + TN}{TP + TN + FP + FN} \quad (1)$$

$$Precision = \frac{TP}{TP + FP} \quad (2)$$

$$Recall = \frac{TP}{TP + FN} \tag{3}$$

$$f_1 \text{ score} = \frac{Precision \times Recall}{Precision + Recall} \tag{4}$$

$$IoU = \frac{Precision \times Recall}{Precision + Recall - (Precision \times Recall)} \tag{5}$$

While accuracy provides a broad measure of correctness, its reliability can be affected by class imbalances within the input data. Precision underscores the model’s capability to accurately recognize relevant objects, while recall assesses its adeptness in capturing all relevant instances. By amalgamating these metrics, their dependence on specific classes is mitigated. The $f_1 \text{ score}$ acts as a safeguard against accuracy inflation due to elevated precision or recall values, as it represents the harmonic mean of both measures [44]. Additionally, the IoU quantifies the ratio of intersecting regions to the total area, acting as a benchmark for evaluating the effectiveness of individual object detection tasks, such as those found in object detection methodologies [45].

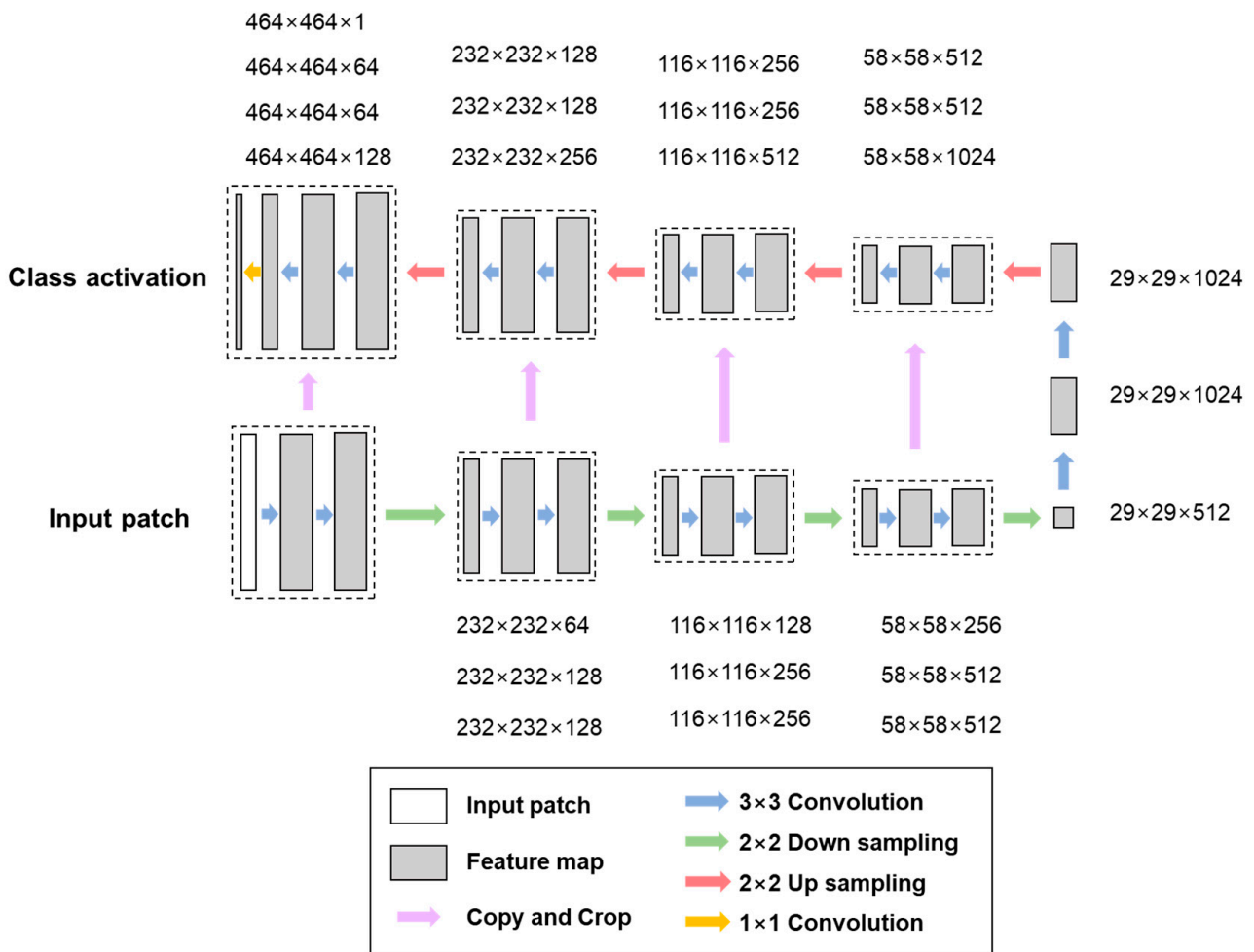


Figure 4. The architecture of U-net-based CNNs.

2.8. Hotspot Analysis

Spatial statistical analysis through hotspot analysis is a methodological approach that delineates geographical clusters, commonly known as hotspots, and dispersed regions, referred to as coldspots, by harnessing the spatial aggregation of surrounding environmental factors such as terrain and geography [46,47].

Within the context of this research, the distinctive distribution patterns of peatland were elegantly represented using the *Getis – Ord* G_i statistical technique, which transforms the data into a standard normalized distribution. Through a meticulous analysis of statistical metrics derived from the temporal evolution of peatland, the study discerned the dynamic alterations in land cover that occurred within the domains of peatland hotspots [48,49]. The formula encapsulated by Equation (6) computes the Z-score pertinent to peatland, with G_i serving as a pivotal component. This equation ingeniously incorporates variables such as \bar{X} to represent the overarching mean of peatland, while S succinctly encapsulates the standard deviation of the mean. Additionally, n stands as the sentinel for the total count of peatlands, while w_j and $w_{i,j}$ symbolize the intricate spatial weighting that defines the interplay between the elements i and j .

$$G_i = \frac{\sum_{j=1}^n w_{i,j}x_j - \bar{X} \sum_{j=1}^n w_{i,j}}{S \sqrt{\frac{n \sum_{j=1}^n w_{i,j}^2 - (\sum_{j=1}^n w_{i,j})^2}{n-1}}}, \bar{X} = \frac{\sum_{j=1}^n x_j}{n}, S = \sqrt{\frac{\sum_{j=1}^n x_j^2}{n} - (\bar{X})^2} \quad (6)$$

Importantly, the captivating realm of Z-scores unfolds with the introduction of a critical significance threshold. Z-scores that surpass the threshold of 1.65 (with a corresponding p -value < 0.10) transition into the domain of hotspots. Within this sphere, peatland exhibits a concentrated distribution. Conversely, situated on the opposite end of this statistical continuum, Z-scores that dip below the threshold of -1.65 (accompanied by a matching p -value < 0.10) earn the designation of coldspots. Within this realm, peatland adopts a dispersed configuration, serving the intricate interplay between spatial variance and the dynamics of the ecological landscape.

3. Results

3.1. CNNs-Based Peatland Classification Using Multi-Temporally Integrated Satellite Imageries

To optimize peatland classification performance, convolutional neural networks (CNNs) were fine-tuned by adjusting key parameters. A patch size of 784×784 was chosen, aligning with prior research by [50]. The number of epochs was incrementally increased from 20 to 50 in steps of 10. The patches per image were scaled from 100 to 250, considering epoch variations. The blur distance was explored between 1 and 8, class weights ranged from 0 to 3, and a loss weight of 0.5 was set, reflecting the peatland's characteristics and Sentinel 2 imageries. After conducting 72 experiments where each parameter was systematically tuned, it was observed that, except for patch size and epoch, the variation in accuracy was within 3%, regardless of other parameter adjustments within their ranges [50].

Precision, representing user accuracy in batch and epoch statistics, serves as a measure of training effectiveness. Notably, in the years 1999, 2009, and 2019, validation accuracy consistently exceeded 93%, with a patch size of 784 and 50 epochs (Table 1). When the patch size was set below 784, CNNs learning showed relatively slower progress in batch and epoch accuracy, precision, and recall. This was accompanied by unstable loss values, suggesting an inadequate patch size for classification (Figure 5). Conversely, with a patch size of 784, efficient training was evident in a batch size below 1000 and with 5 epochs. The application of diverse data augmentation methods, such as rotation and flip, was effective at the specified patch size.

Table 1. Epoch validation statistics of peatland classification using CNNs at the last epoch.

Year	Overall Accuracy	Validation Loss	Validation Precision	Validation Recall	F_1 Score	IoU
1999	0.939	0.113	0.654	0.618	0.318	0.466
2009	0.948	0.118	0.680	0.649	0.332	0.497
2019	0.952	0.146	0.690	0.653	0.335	0.505

The classification results for the years 1999, 2009, and 2019 yielded accuracy rates of 93.9%, 94.8%, and 95.2%, respectively. However, the recall values were relatively lower, at 61.8%, 64.9%, and 65.3%. This suggests potential overfitting due to noise issues in two-dimensional satellite imagery, which lacks the depth information (x, y). Thus, future research should focus on optimizing model architectures and consider incorporating three-dimensional data, such as RADAR, to adjust thresholds.

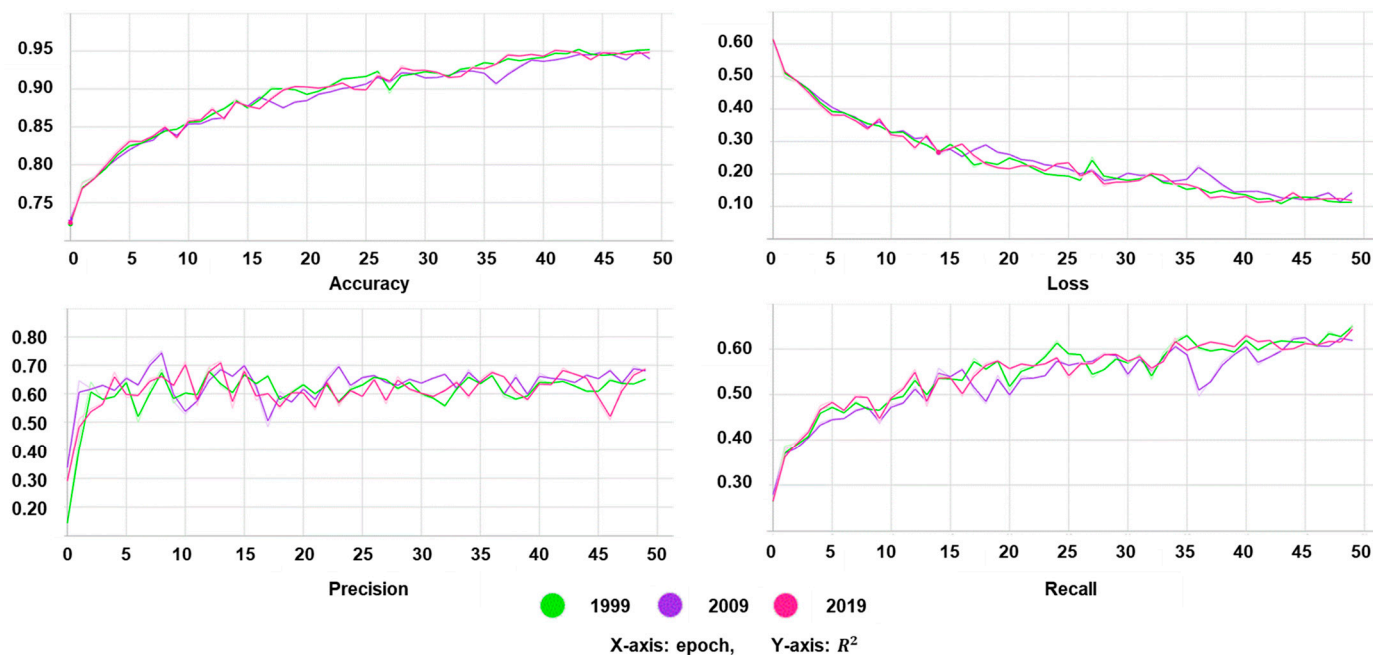


Figure 5. Epoch validation statistics of CNNs model operation.

Upon analyzing Figure 6, a conspicuous declining pattern in peatland coverage from 1999 to 2019 becomes apparent. The expansive OKI region encompasses a total area of 17,907 km². Within this expanse, an area spanning 8226 km² was designated as peatland in 1999, and remarkably, 80.29% of this originally identified peatland area persisted as such in 2019. This persistence underscores the resilience of the peatland landscape.

Intriguingly, the shifting dynamics of peatland classifications shed light on notable transitions. Approximately 37.32% of the initially classified 8226 km² of peatland underwent changes, transitioning either to “suspected area of peatland” or to “no peatland” categories. This underscores the evolving nature of these areas, and highlights the intricacies of their land cover shifts.

Delving further, within the original “suspected area of peatland” category encompassing 3979 km², a substantial 31.80% area experienced a transformation to the “no peatland” classification. This transition could be attributed to a multitude of factors, including changing environmental conditions, land use alterations, and natural processes. The interplay of these factors underscores the dynamic nature of peatland ecosystems and the complexities involved in their classification changes over time.

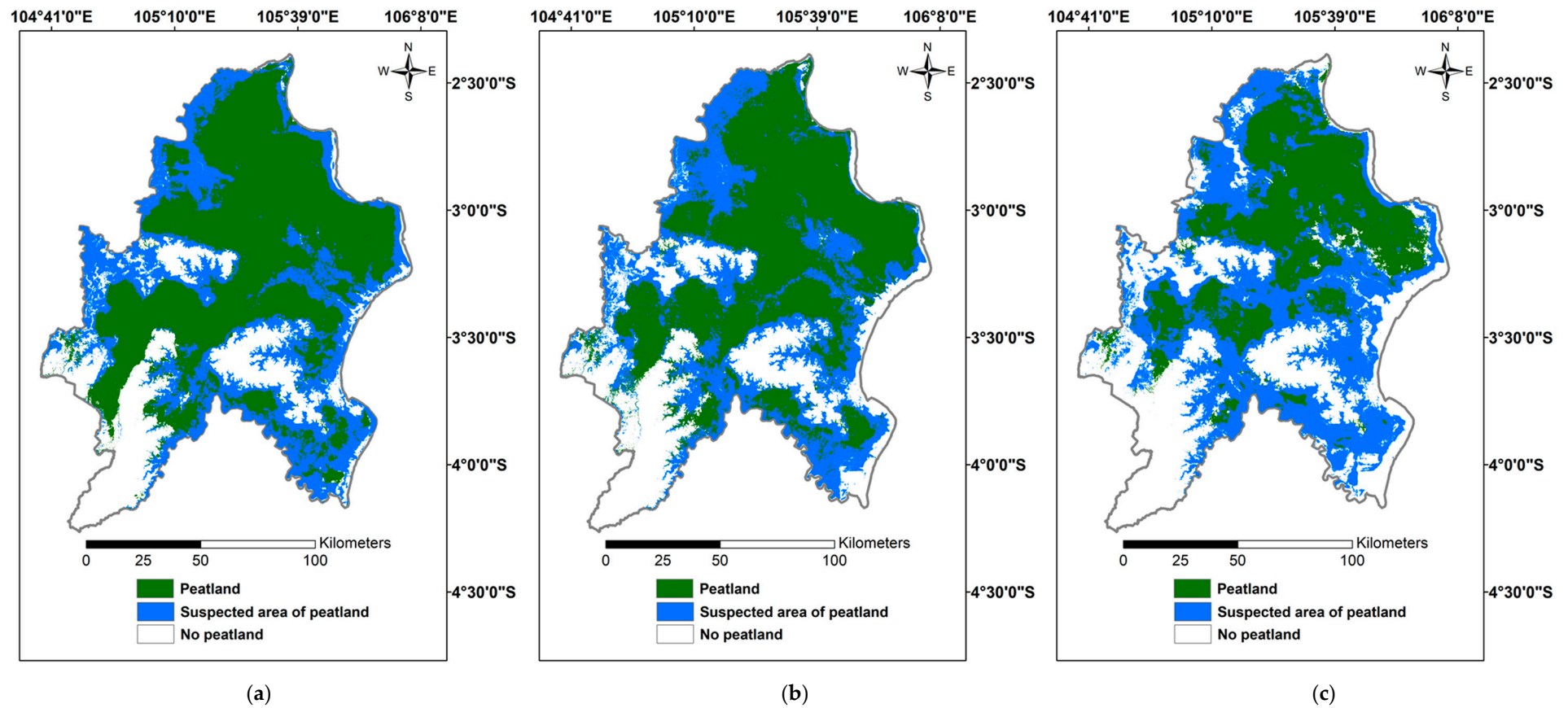


Figure 6. Past peatland classification map using CNNs with the highest accuracy. (a) Peatland classification map of 1999; (b) Peatland classification map of 2009; (c) Peatland classification map of 2019.

The term “suspected area of peatland” encapsulates a certain level of ambiguity owing to its dual interpretation, potentially signifying the presence or absence of peatland characteristics. To address this ambiguity, a meticulous methodology was devised and executed in this study, leveraging the wealth of data gathered from field surveys conducted in 2011 and 2019. Specifically, this study employed a stringent criterion for classifying areas as “peatland”. Such classification was granted exclusively to those areas demonstrating consistent peatland characteristics in both the 2011 and 2019 surveys. In contrast, regions that exhibited peatland attributes in either the 2011 or 2019 survey were designated as “suspected areas of peatland”. This nuanced approach underscored the need for a comprehensive characterization of peatland attributes across both survey years to unequivocally classify an area as “peatland”. Such an approach aimed to mitigate any potential misclassifications arising from singular instances of peatland-like features.

However, it is imperative to acknowledge that further refinement of the “suspected area of peatland” category can be achieved through the integration of additional reference data. Future research endeavors employing such supplementary data hold the potential to offer a more precise classification of these ambiguous areas. This, in turn, is expected to foster the development of an enhanced peatland classification model, one founded on a more rigorous classification of the suspected peatland areas. The ramifications of this meticulous classification methodology are substantial. It not only contributes to a more accurate understanding of peatland dynamics, but also holds the promise of bolstering the accuracy of peatland classification models. By strategically delineating areas of certain ambiguity, the study sets the stage for improved decision-making processes concerning land-use planning, conservation efforts, and ecosystem management. Ultimately, this approach aligns with the broader goal of harnessing the power of geospatial technologies for sustainable and informed environmental management.

3.2. Land Cover Changes in Peatlands

According to past peatland classification results from the CNNs model, the area classified as peatland decreased from 8226 km² in 1999 to 7770 km² in 2009, and ultimately to 5156 km² in 2019. This indicates that approximately 37.32% of peatland transitioned into the suspected area of peatland or no peatland. In this study, we quantitatively assessed how the land cover types of peatland changed into other covers. Among the categories that showed changes exceeding 5% of the total area from 1999 to 2019, estate plantations and swamp shrubs stood out. The area of estate crop plantation increased from 140 km² (1.70%) in 1999 to 463 km² (8.98%) in 2019, while plantation forest expanded from 0 km² (0.00%) to 2764 km² (53.61%) during the same period. In contrast, swamp shrub decreased from 5656 km² (68.76%) to 1196 km² (23.19%), representing a 45.57% reduction. Notably, a significant portion of the reduced peatland was classified as swamp shrub (Figure 7). However, this study did not investigate the direct causes of land cover changes in peatland. To understand the reasons behind these changes, further research is needed.

Land cover changes in peatlands are driven by a combination of natural processes influenced by hydrological patterns, climate, and vegetation succession, as well as human activities. Variations in precipitation and temperature have led to fluctuations in water levels, affecting the distribution and composition of land cover types. Human activities, particularly the conversion of forested areas into agricultural landscapes dominated by palm oil plantations, have significantly impacted land cover changes. This conversion, involving deforestation and the expansion of agricultural activities, has resulted in shifts in land cover categories. The establishment of industrial plantations, such as oil palm and acacia pulpwood, has also left its mark on peatland landscapes. This transformation often includes drainage and hydrological adjustments, leading to a shift from diverse ecosystems to monoculture plantations. Urbanization and infrastructure development have contributed to changes in land cover patterns as well. Peatlands being converted into urban spaces or utilized for infrastructure have directly influenced land cover changes.

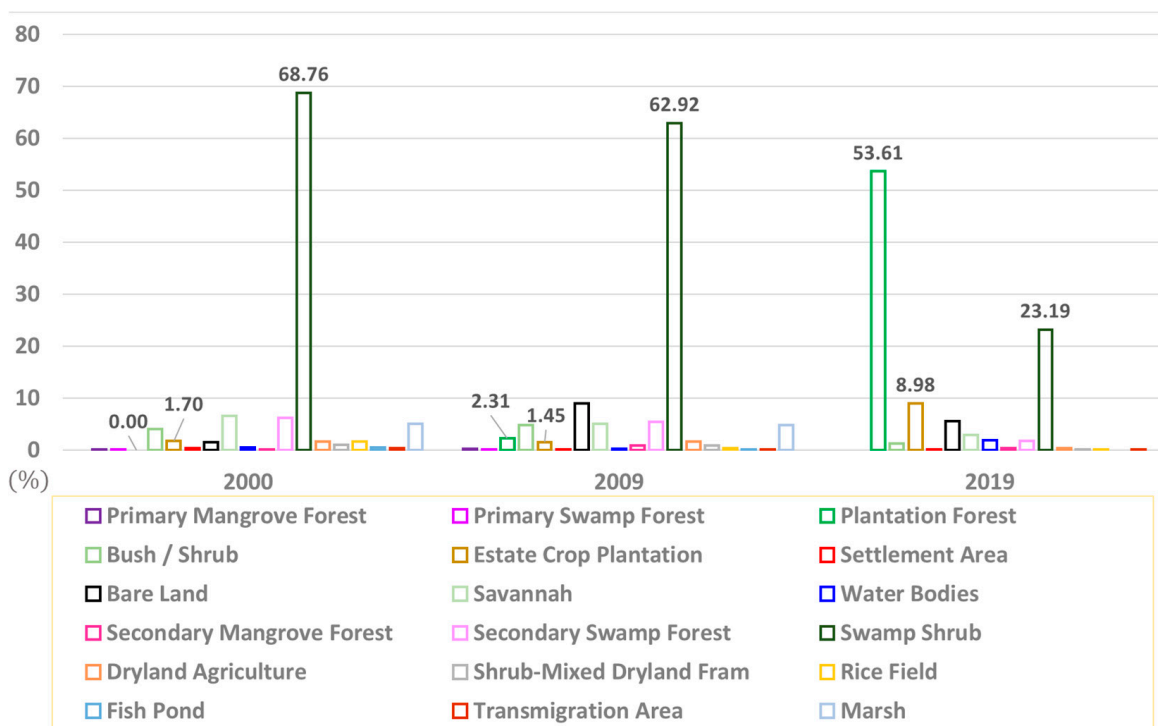


Figure 7. Time-series land cover change statistics in peatlands of the OKI region in Indonesia.

The complex interplay between natural dynamics and human interventions over two decades has shaped evolving land cover patterns in Indonesian peatlands. These transformations have significant implications for land use strategies, resource management, and environmental preservation.

3.3. Changes in Land Cover and Peatland Distribution in Fire Occurrence Hotspots

As with all wildland fires, peatlands burn when an ignition event occurs in the presence of fuel and the right conditions to support combustion. Furthermore, the role of fire incidents, whether deliberately set or accidental, cannot be underestimated in shaping land cover. These fire events have the potential to modify the composition of vegetation, transitioning once-forested or shrubby terrains into open, charred landscapes.

The wildland fires not only change the above-ground landscape, but also release carbon stored in the soil [3]. Covering the years 2000 to 2009, a total of 17,503 fire incidents were recorded, with 13.00% of them transitioning from peatland to either peatland-suspected areas or non-peatland areas. Shifting our focus to the timeframe from 2010 to 2019, 30,357 fire occurrences were registered, and 30.23% of these cases saw a change from peatland to peatland-suspected areas or non-peatland areas. Over the entire period from 2000 to 2019, a total of 47,860 direct or indirect fire incidents were documented, with 23.93% experiencing a shift from peatland to peatland-suspected areas or non-peatland areas. To assert that fire has a direct impact on peatland loss would require additional in-depth analysis. However, when examining the overall statistics, it becomes evident that the areas where fires have occurred show a substantial peatland loss rate. The gray area in Figure 8 represents the regions where the fires occurred from 2000 to 2019, and the red portions marked as hotspots indicate concentrated fire incidents.

The land cover situation in 2020 raises the need to comprehend the current status in areas with hotspots. A total of 7470 hotspots were identified with a confidence level of 90% or higher. Among these, 6678 points (89.16%) were categorized as plantation forest, 151 points (2.02%) as bush and shrub, 428 points (5.71%) as estate crop plantation, 183 points (2.44%) as secondary swamp forest, 11 points (0.15%) as dryland agriculture, and 19 points (0.25%) as shrub-mixed dryland farm.

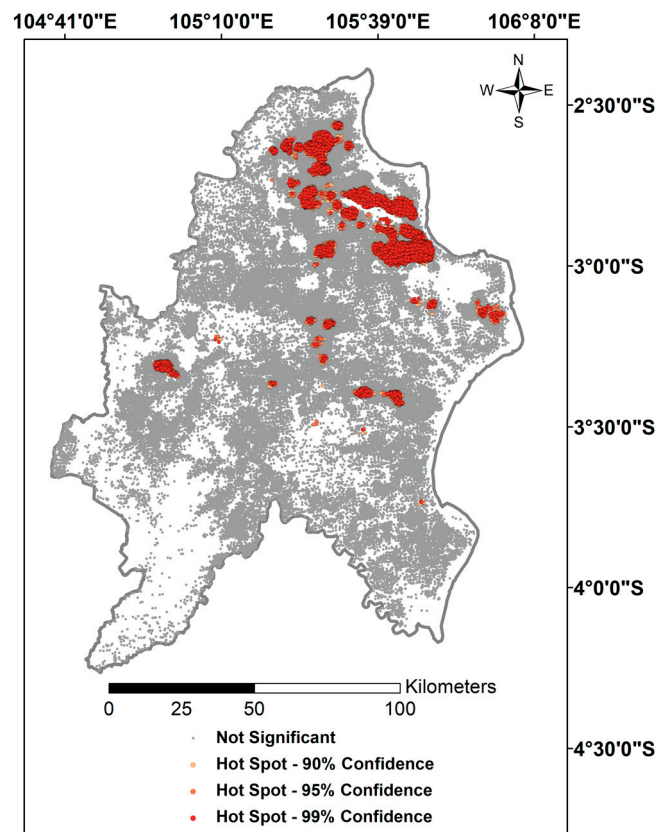


Figure 8. Map of fire occurrence hotspots in the OKI region.

4. Discussion

To highlight the originality of our research, we conducted a comparative analysis of our peatland classification outcomes with those of other studies (Table 2).

Table 2. Comparison of peatland/wetland classification models in current and previous studies.

Region	Overall Accuracy (OA)	Model *	Type of Dataset	Spatial Resolution (m)	Sources
Ogan Komering Ilir, Indonesia	0.939–0.952	U-net CNNs	Satellite with multispectral bands	10	This study
Alberta, Canada	0.802	U-net CNNs	Satellite with multispectral bands and SAR	10	[51]
Alberta, Canada	0.870	BRT	Satellite with multispectral bands and SAR	10	[52]
Ogan Komering Ilir, Indonesia	0.706	RF	Satellite with multispectral bands	500	[53]
	0.727	GB			
	0.740	XGB			
	0.755	CatB			
	0.737	DL			
Riau, Indonesia	0.550–0.760	DTC	Satellite with multispectral bands and SAR	30	[54]
Sumatra and Kalimantan, Indonesia	0.907–0.911	DTC	Satellite with multispectral bands and SAR	30	[55]

* SAR: synthetic aperture radar; BRT: boosted regression tree; RF: random forest; GB: gradient boosting; XGB: extreme gradient boosting; CatB: categorical boosting; DL: deep learning; DTC: decision tree classifier.

Ref. [51] demonstrated the effectiveness of deep convolutional neural networks (CNNs) in large-scale remote sensing landcover classifications, specifically addressing challenges in wetland classes defined by the Canadian Wetland Classification System. The comparison with the conventional XGBoost algorithm underscored the superior accuracy of CNN-based classifications, indicating its potential for large-scale wetland inventory generation. In study [52], the focus on utilizing freely available satellite data and cloud-computing platforms for mapping peatlands in Alberta, Canada, resulted in an impressive 87% accuracy in distinguishing peatlands from mineral wetlands. This data-driven framework holds promise for geopolitical-scale wetland and landcover inventories, supporting responsible resource management. Ref. [53] emphasized the critical role of peatlands in global climate regulation, utilizing Landsat 8 OLI and MODIS data alongside machine learning (ML) and deep learning (DL) methods for accurate delineation. The effectiveness of the Cat Boosting algorithm in achieving high accuracy delineation results suggests its potential for broader landcover mapping applications. In the study by [54], mapping tropical peatlands in Indonesia using phased array type L-band synthetic aperture radar (PALSAR) data, particularly incorporating dual-polarization and fully polarimetric data, demonstrated a 76% overall accuracy. Notably, the inclusion of the “distance to river” feature enhanced the proposed methodology’s efficiency, especially in a region undergoing extensive land-use changes. Adding to this discussion, Ref. [55] focused on mapping Indonesia’s wetland cover, encompassing peatlands, freshwater wetlands, and mangroves as a unified thematic class. Their approach, utilizing expert-interpreted training data and diverse data inputs, generated a national-scale wetland map at a 60 m spatial resolution. The resulting map, covering 21.0% of Indonesia’s land, demonstrated an 89% overall agreement with existing products, providing an internally consistent algorithm-derived wetland extent map useful for quantifying land conversion rates within and outside wetlands. This aligns with our broader discussion on advancing remote sensing techniques and emphasizing the pivotal role of peatlands in diverse geographic contexts. Due to the limited global research on peatland classification, this study conducted a comparative analysis with several wetland classification studies in areas similar to peatlands [51–55]. Despite not utilizing SAR data with elevation information, our study achieved high spatial resolution and accuracy. This suggests that the accuracy could potentially be further improved if additional RADAR or LiDAR information is incorporated into our research.

Despite the promising outcomes demonstrated by U-net models across various applications, their efficacy in specific locales may encounter certain constraints. A primary hurdle involves the adequacy and representativeness of the training dataset. Should the training dataset predominantly comprise samples from a specific geographical region or lack diversity in peatland composition, the model’s generalization capacity to novel and unexplored areas could be compromised. To surmount this limitation and enhance the U-net models’ performance, several strategies warrant consideration.

An effective approach involves broadening the training dataset to encompass a more varied array of samples from diverse regions, thereby augmenting the model’s proficiency in capturing variations in peatland characteristics. This may entail the acquisition of additional ground truth data or harnessing existing datasets from a broader geographic and climatic spectrum. Additionally, the integration of transfer learning techniques proves beneficial. Preliminary training of the U-net model on an extensive and diverse dataset, such as a global peatland map, followed by fine-tuning with region-specific data, allows the model to leverage knowledge derived from broader contexts while adapting to the distinct characteristics of the target region. Furthermore, the judicious selection of the patch size for analysis assumes paramount importance. While larger patch sizes have the potential to capture more contextual information and potentially enhance accuracy, they may concurrently pose challenges in terms of computational resources and processing time. Thus, it is imperative to factor in available hardware resources and computational constraints when determining the optimal patch size. Striking a delicate balance between accuracy and practical limitations is essential to ensure efficient and effective analysis.

While U-net-based CNNs models exhibit significant promise for peatland classification, their performance in specific regions may be circumscribed by the narrow focus on the target area. Addressing challenges pertaining to training data representation, integrating transfer learning techniques and prudently selecting patch sizes can augment the accuracy and generalizability of U-net models. This, in turn, facilitates more robust and accurate analysis of tree species in geographically restricted regions.

5. Conclusions

This study employed convolutional neural networks (CNNs) to optimize peatland classification performance by fine-tuning key parameters, ultimately achieving accurate results. A patch size of 784×784 —as inspired by prior research—along with 50 epochs demonstrated the best classification outcomes, consistently exceeding 93% accuracy in validation for the years 1999, 2009, and 2019. Analyzing the broader picture of peatland dynamics over two decades, our findings revealed significant changes in land cover. Approximately 37.32% of the initially classified peatland area transitioned to suspected peatland areas or no peatland, with estate plantation and swamp shrub showing notable shifts. Human activities, such as agricultural conversions, urbanization, and infrastructure development, have significantly influenced these land cover changes alongside natural processes. The wildland fires played a pivotal role in shaping land cover in peatlands, with approximately 23.93% of fire incidents leading to shifts from peatland to suspected peatland or non-peatland areas. While confirming a direct causal link between fires and peatland loss necessitates additional analysis, the correlation between areas affected by fires and the rates of peatland loss is remarkably evident. Furthermore, the study addressed the ambiguity surrounding the “suspected area of peatland” category by developing a meticulous classification methodology, combining field surveys from 2011 and 2019. This approach offers a comprehensive characterization of peatland attributes, enhancing our understanding of peatland dynamics and classification accuracy. The implications of this research extend beyond academia. The precise classification methodology provides a foundation for improved land-use planning, conservation efforts, and ecosystem management. As we navigate the complex interplay between natural dynamics and human interventions, these findings serve as a valuable resource for sustainable environmental management in Indonesian peatlands.

Author Contributions: S.C. developed overall concept and methodology. S.C. conducted analysis, J.L. (Junghee Lee) processed data. J.L. (Joongbin Lim); E.C. supervised overall research. All authors have read and agreed to the published version of the manuscript.

Funding: This research was funded by National Institute of Forest Science grant number [FM0800-2021-03-2023 and FM0103-2021-01-2023].

Data Availability Statement: Data are contained within the article.

Acknowledgments: The authors would like to thank the anonymous reviewers and editorial staff for their comments, which greatly improved this manuscript.

Conflicts of Interest: The authors declare no conflict of interest.

References

1. Yu, Z.; Loisel, J.; Brosseau, D.P.; Beilman, D.W.; Hunt, S.J. Global peatland dynamics since the Last Glacial Maximum. *Geophys. Res. Lett.* **2010**, *37*, L13402. [[CrossRef](#)]
2. Scharlemann, J.P.; Tanner, E.V.; Hiederer, R.; Kapos, V. Global soil carbon: Understanding and managing the largest terrestrial carbon pool. *Carbon Manag.* **2014**, *5*, 81–91. [[CrossRef](#)]
3. Turetsky, M.R.; Benscoter, B.; Page, S.; Rein, G.; Van Der Werf, G.R.; Watts, A. Global vulnerability of peatlands to fire and carbon loss. *Nat. Geosci.* **2015**, *8*, 11–14. [[CrossRef](#)]
4. Wilkinson, S.L.; Andersen, R.; Moore, P.A.; Davidson, S.J.; Granath, G.; Waddington, J.M. Wildfire and degradation accelerate northern peatland carbon release. *Nat. Clim. Chang.* **2023**, *13*, 456–461. [[CrossRef](#)]

5. Field, R.D.; Van Der Werf, G.R.; Fanin, T.; Fetzer, E.J.; Fuller, R.; Jethva, H.; Levy, R.; Livesey, M.J.; Luo, M.; Torres, O.; et al. Indonesian fire activity and smoke pollution in 2015 show persistent nonlinear sensitivity to El Niño-induced drought. *Proc. Natl. Acad. Sci. USA* **2016**, *113*, 9204–9209. [[CrossRef](#)]
6. Margono, B.A.; Potapov, P.V.; Turubanova, S.; Stolle, F.; Hansen, M.C. Primary forest cover loss in Indonesia over 2000–2012. *Nat. Clim. Chang.* **2014**, *4*, 730–735. [[CrossRef](#)]
7. Miettinen, J.; Shi, C.; Liew, S.C. Land cover distribution in the peatlands of Peninsular Malaysia, Sumatra and Borneo in 2015 with changes since 1990. *Glob. Ecol. Conserv.* **2016**, *6*, 67–78. [[CrossRef](#)]
8. Austin, K.G.; Schwantes, A.; Gu, Y.; Kasibhatla, P.S. What causes deforestation in Indonesia? *Environ. Res. Lett.* **2019**, *14*, 024007. [[CrossRef](#)]
9. Medrilzam, M.; Smith, C.; Aziz, A.A.; Herbohn, J.; Dargusch, P. Smallholder farmers and the dynamics of degradation of peatland ecosystems in Central Kalimantan, Indonesia. *Ecol. Econ.* **2017**, *136*, 101–113. [[CrossRef](#)]
10. Irfan, M.; Koriyanti, E.; Ariani, M.; Sulaiman, A.; Iskandar, I. Determination of soil moisture reduction rate on peatlands in South Sumatra due to the 2019 extreme dry season. *IOP Conf. Ser. Earth Environ. Sci.* **2021**, *713*, 012025. [[CrossRef](#)]
11. Prasetyo, L.B.; Setiawan, Y.; Condro, A.A.; Kustiyo, K.; Putra, E.I.; Hayati, N.; Wijayanto, A.K.; Ramadhi, A.; Murdiyarso, D. Assessing Sumatran Peat Vulnerability to Fire under Various Condition of ENSO Phases Using Machine Learning Approaches. *Forests* **2022**, *13*, 828. [[CrossRef](#)]
12. Poggio, L.; Lassauce, A.; Gimona, A. Modelling the extent of northern peat soil and its uncertainty with sentinel: Scotland as example of highly cloudy region. *Geoderma* **2019**, *346*, 63–74. [[CrossRef](#)]
13. Melton, J.R.; Chan, E.; Millard, K.; Fortier, M.; Winton, R.S.; Martín-López, J.M.; Cadillo-Quiroz, H.; Kidd, D.; Verchot, L.V. A map of global peatland extent created using machine learning (Peat-ML). *Geosci. Model Dev.* **2022**, *15*, 4709–4738. [[CrossRef](#)]
14. Xu, J.; Morris, P.J.; Liu, J.; Holden, J. PEATMAP: Refining estimates of global peatland distribution based on a meta-analysis. *Catena* **2018**, *160*, 134–140. [[CrossRef](#)]
15. Minasny, B.; Berglund, Ö.; Connolly, J.; Hedley, C.; de Vries, F.; Gimona, A.; Kempen, B.; Kidd, D.; Lilja, H.; Malone, B.; et al. Digital mapping of peatlands—A critical review. *Earth-Sci. Rev.* **2019**, *196*, 102870. [[CrossRef](#)]
16. Anda, M.; Ritung, S.; Suryani, E.; Hikmat, M.; Yatno, E.; Mulyani, A.; Subandiono, R.E. Revisiting tropical peatlands in Indonesia: Semi-detailed mapping, extent and depth distribution assessment. *Geoderma* **2021**, *402*, 115235. [[CrossRef](#)]
17. Wu, Y.; Chan, E.; Melton, J.R.; Versegny, D.L. A map of global peatland distribution created using machine learning for use in terrestrial ecosystem and earth system models. *Geosci. Model Dev. Discuss.* **2017**, 1–21. [[CrossRef](#)]
18. Hadiyani, F.S.; Nurhayati, A.D. Hotspot analysis in 2015 and 2019 at ogan komering ilir district south Sumatera province. *IOP Conf. Ser. Earth Environ. Sci.* **2022**, *959*, 012056. [[CrossRef](#)]
19. Rendana, M.; Idris, W.M.R.; Rahim, S.A.; Abdo, H.G.; Almohamad, H.; Al Dughairi, A.A.; Albanai, J.A. Current and future land fire risk mapping in the southern region of Sumatra, Indonesia, using CMIP6 data and GIS analysis. *SN Appl. Sci.* **2023**, *5*, 210. [[CrossRef](#)]
20. Rouse, J.W.; Haas, R.H.; Schell, J.A.; Deering, D.W. Monitoring vegetation systems in the Great Plains with ERTS. *NASA Spec. Publ.* **1974**, *351*, 309.
21. Gao, B.C. NDWI—A normalized difference water index for remote sensing of vegetation liquid water from space. *Remote Sens. Environ.* **1996**, *58*, 257–266. [[CrossRef](#)]
22. McFeeters, S.K. The use of the Normalized Difference Water Index (NDWI) in the delineation of open water features. *Int. J. Remote Sens.* **1996**, *17*, 1425–1432. [[CrossRef](#)]
23. Haboudane, D.; Miller, J.R.; Tremblay, N.; Zarco-Tejada, P.J.; Dextraze, L. Integrated narrow-band vegetation indices for prediction of crop chlorophyll content for application to precision agriculture. *Remote Sens. Environ.* **2002**, *81*, 416–426. [[CrossRef](#)]
24. Huete, A.; Didan, K.; Miura, T.; Rodriguez, E.P.; Gao, X.; Ferreira, L.G. Overview of the radiometric and biophysical performance of the MODIS vegetation indices. *Remote Sens. Environ.* **2002**, *83*, 195–213. [[CrossRef](#)]
25. Huete, A.R. A soil-adjusted vegetation index (SAVI). *Remote Sens. Environ.* **1988**, *25*, 295–309. [[CrossRef](#)]
26. Key, C.H.; Benson, N.; Ohlen, D.; Howard, S.; McKinley, R.; Zhu, Z. The Normalized Burn Ratio and Relationships to Burn Severity: Ecology, Remote Sensing and Implementation. In Proceedings of the Ninth Biennial Remote Sensing Applications Conference, San Diego, CA, USA, 8–12 April 2002.
27. Qi, J.; Chehbouni, A.; Huete, A.R.; Kerr, Y.H.; Sorooshian, S. A modified soil adjusted vegetation index. *Remote Sens. Environ.* **1994**, *48*, 119–126. [[CrossRef](#)]
28. Czapiewski, S. Assessment of the Applicability of UAV for the Creation of Digital Surface Model of a Small Peatland. *Front. Earth Sci.* **2022**, *10*, 834923. [[CrossRef](#)]
29. Pflugmacher, D.; Krankina, O.N.; Cohen, W.B. Satellite-based peatland mapping: Potential of the MODIS sensor. *Glob. Planet. Chang.* **2007**, *56*, 248–257. [[CrossRef](#)]
30. Limpens, J.; Berendse, F.; Blodau, C.; Canadell, J.G.; Freeman, C.; Holden, J.; Roulet, N.; Rydin, H.; Schaepman-Strub, G. Peatlands and the carbon cycle: From local processes to global implications—A synthesis. *Biogeosciences* **2008**, *5*, 1475–1491. [[CrossRef](#)]
31. Buffam, I.; Carpenter, S.R.; Yeck, W.; Hanson, P.C.; Turner, M.G. Filling holes in regional carbon budgets: Predicting peat depth in a north temperate lake district. *J. Geophys. Res. Biogeosci.* **2010**, *115*, G01005. [[CrossRef](#)]
32. Xing, W.; Bao, K.; Gallego-Sala, A.V.; Charman, D.J.; Zhang, Z.; Gao, C.; Lu, X.; Wang, G. Climate controls on carbon accumulation in peatlands of Northeast China. *Quat. Sci. Rev.* **2015**, *115*, 78–88. [[CrossRef](#)]

33. Altmann, A.; Toloşi, L.; Sander, O.; Lengauer, T. Permutation importance: A corrected feature importance measure. *Bioinformatics* **2010**, *26*, 1340–1347.2.3. [[CrossRef](#)]
34. Sulaeman, Y.; Mulyani, A.; Wahyunto, M.S. *Mapping Soil Depth Characteristics Using Digital Soil Mapping Techniques to Monitor Land Degradation*; Asia-Pacific Economic Cooperation: Chiang Mai, Thailand, 2013.
35. Wahyunto, R.S.; Suparto, S.H. *Map of Peatland Distribution and Its C Content in Kalimantan*; Wetlands International-Indonesia Programme and Wildlife Habitat Canada: Bogor, Indonesia, 2004.
36. Wahyunto, H.B.; Bekti, H.; Widiastuti, F. *Maps of Peatland Distribution, Area and Carbon Content in Papua, 2000–2001*; Wetlands International-Indonesia Programme & Wildlife Habitat Canada: Bogor, Indonesia, 2006.
37. Wahyunto, S.R.; Nugroho, K.; Sulaeman, Y.; Hikmatullah, C.T.; Suparto, S. *Peta Lahan Gambut Terdegradasi Pulau Kalimantan dan Papua [Degraded Peatland Map for Kalimantan dan Papua]*; Indonesia Climate Change Trust Fund (ICCTF)–Bappenas, Agency for Agricultural Research and Development, Ministry of Agriculture: Jakarta, Indonesia, 2013.
38. Balai Besar Penelitian dan Pengembangan Sumber Daya Lahan Pertanian (BBSDLP). *Peta Lahan Gambut Indonesia 1: 250,000*; BBSDLP: Bogor, Indonesia, 2011.
39. Balai Besar Penelitian dan Pengembangan Sumber Daya Lahan Pertanian (BBSDLP). *Peta Lahan Gambut Indonesia 1: 50,000*; BBSDLP: Bogor, Indonesia, 2019.
40. Giglio, L.; Schroeder, W.; Hall, J.V.; Justice, C.O. *MODIS Collection 6 Active Fire Product User's Guide Revision A*; Department of Geographical Sciences, University of Maryland: College Park, MD, USA, 2015; p. 9.
41. Indonesian Ministry of Environment and Forestry (MoEF). *Petunjuk Teknis: Penafsiran Citra Satelit Resolusi Sedang Untuk Update Data Penutupan Lahan Nasional*; MoEF: Jakarta, Indonesia, 2020.
42. Ronneberger, O.; Fischer, P.; Brox, T. U-net: Convolutional Networks for Biomedical Image Segmentation. In Proceedings of the Medical Image Computing and Computer-Assisted Intervention—MICCAI 2015: 18th International Conference, Munich, Germany, 5–9 October 2015.
43. Cha, S.; Jo, H.W.; Kim, M.; Song, C.; Lee, H.; Park, E.; Lim, J.; Schepaschenko, D.; Shvidenko, A.; Lee, W.K. Application of deep learning algorithm for estimating stand volume in South Korea. *J. Appl. Remote Sens.* **2022**, *16*, 024503. [[CrossRef](#)]
44. Yang, Y. An evaluation of statistical approaches to text categorization. *Inf. Retr.* **1999**, *1*, 69–90. [[CrossRef](#)]
45. Wilks, Y.; Fass, D.; Guo, C.M.; McDonald, J.E.; Plate, T.; Slator, B.M. Providing machine tractable dictionary tools. *Mach. Transl.* **1990**, *5*, 99–154. [[CrossRef](#)]
46. Cáceres, C.F. Using GIS in hotspots analysis and for forest fire risk zones mapping in the Yeguaré Region, Southeastern Honduras. *Pap. Resour. Anal.* **2011**, *13*, 1–14.
47. Brown, K.A.; Parks, K.E.; Bethell, C.A.; Johnson, S.E.; Mulligan, M. Predicting plant diversity patterns in Madagascar: Understanding the effects of climate and land cover change in a biodiversity hotspot. *PLoS ONE* **2015**, *10*, e0122721. [[CrossRef](#)] [[PubMed](#)]
48. Ebdon, D. *Statistics in Geography Second Edition: A Practical Approach*; Blackwell Publishing: Malden, MA, USA, 1985.
49. Getis, A.; Ord, J.K. The analysis of spatial association by use of distance statistics. *Geogr. Anal.* **1992**, *24*, 189–206. [[CrossRef](#)]
50. Cha, S.; Lim, J.; Kim, K.; Yim, J.; Lee, W.K. Deepening the Accuracy of Tree Species Classification: A Deep Learning-Based Methodology. *Forests* **2023**, *14*, 1602. [[CrossRef](#)]
51. De Lancey, E.R.; Simms, J.F.; Mahdianpari, M.; Brisco, B.; Mahoney, C.; Kariyeva, J. Comparing deep learning and shallow learning for large-scale wetland classification in Alberta, Canada. *Remote Sens.* **2019**, *12*, 2. [[CrossRef](#)]
52. De Lancey, E.R.; Kariyeva, J.; Bried, J.T.; Hird, J.N. Large-scale probabilistic identification of boreal peatlands using Google Earth Engine, open-access satellite data, and machine learning. *PLoS ONE* **2019**, *14*, e0218165.
53. Sencaki, D.B.; Prayogi, H.; Arfah, S.; Pianto, T.A. Machine learning approach for peatland delineation using multi-sensor remote sensing data in Ogan Komering Ilir Regency. *IOP Conf. Ser. Earth Environ. Sci.* **2020**, *500*, 012005. [[CrossRef](#)]
54. Novresiandi, D.A.; Nagasawa, R. Polarimetric synthetic aperture radar application for tropical peatlands classification: A case study in Siak River Transect, Riau Province, Indonesia. *J. Appl. Remote Sens.* **2017**, *11*, 016040. [[CrossRef](#)]
55. Margono, B.A.; Bwangoy, J.R.B.; Potapov, P.V.; Hansen, M.C. Mapping wetlands in Indonesia using Landsat and PALSAR data-sets and derived topographical indices. *Geo-Spat. Inf. Sci.* **2014**, *17*, 60–71. [[CrossRef](#)]

Disclaimer/Publisher's Note: The statements, opinions and data contained in all publications are solely those of the individual author(s) and contributor(s) and not of MDPI and/or the editor(s). MDPI and/or the editor(s) disclaim responsibility for any injury to people or property resulting from any ideas, methods, instructions or products referred to in the content.